



Dynamics of Carbon Dioxide Breakthrough in a Carbon Monolith Over a Wide Concentration Range

HYUNGWOONG AHN AND STEFANO BRANDANI*

Department of Chemical Engineering, University College London, Torrington Place, London WC1E 7JE, UK

s.brandani@ucl.ac.uk

Abstract. Monoliths, and structured column packings in general, offer the advantage of allowing increased throughput and reduced pressure drops. The performance of a monolith is commonly based on models of an equivalent characteristic channel representative of the system. The HETP or the dispersion of a breakthrough curve are indicative of the separation efficiency of an adsorption column, and what is typically observed is that the experimental results are below expectation. We present a detailed model that we have developed recently, which takes into account the distribution of the size of the monolith channels, the distribution of the wall thicknesses as well as the number of monolith sections in the column. In this contribution, the mathematical model is extended to include nonlinear isotherms and a procedure to determine the equilibrium parameters from a modified moment equation is applied to characterise the system CO₂ on a carbon based monolith. Model predictions, based on independently measured kinetic parameters, are shown to provide an excellent match to the experimental results over a wide range of gas phase concentrations.

Keywords: monolith, carbon dioxide, breakthrough, HETP

1. Introduction

Structured adsorbents can increase the performance of separation units when compared to traditional packed columns (Ruthven and Thaeron, 1996). Monoliths are particularly suitable for rapid cycle pressure swing adsorption (PSA), VOC removal, desiccant cooling and other processes where pressure drop has a significant economic impact (Ruthven, 2000). Typically, in order to design these units the performance of an individual representative channel is considered and the theory of Golay (1958) is applied. To improve this approach, Ahn and Brandani (2004a) have developed a 3-D model for gas and liquid phase adsorption in a square or rectangular channel, and have derived a simple HETP equation that takes into account the effect of the solid material in the four corners. Even with this new correction, it is still not possible to fully reconcile the breakthrough

results on a carbon monolith and ZLC experiments on a fragment of the monolith presented by Brandani et al. (2004). The experimental dispersion of the breakthrough curves is significantly larger than that which would be predicted from the diffusional time constant extracted from the ZLC experiments. This has led us to investigate the effect of the channel size distribution and the wall thickness distribution on the performance of a monolith, and the general model (Ahn and Brandani, 2004b) indicates that these have a significant effect, as well as the number of sections in a column.

To preserve the integrity of the monolith, the simplest way to measure an adsorption isotherm is using breakthrough experiments. In this contribution, we present an application of the procedure to determine the adsorption isotherm from integral step breakthrough experiments (Brandani, 2004), which allows us to extend our general model to include non-linear equilibrium effects and compare the model predictions with experimental results over a wide range of CO₂ concentrations.

*Holder of the Royal Society/Wolfson Research Merit Award.

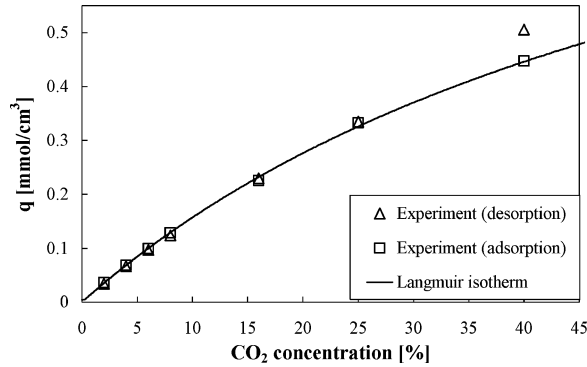


Figure 1. Carbon dioxide isotherm at 298 K and atmospheric pressure.

2. Equilibrium Isotherm

The adsorption equilibrium of carbon dioxide in a carbon monolith was obtained in the range of 2% to 40% CO_2 from the adsorption and desorption breakthrough experiments at atmospheric conditions. Nitrogen was used as a carrier gas in a system where sorbate flowrate can be switched on and off using a three way valve. The operating conditions of the breakthrough experiments and the detailed dimensions of the column are listed in Table 1.

Given the large concentration steps, the equilibrium properties were calculated including a flowrate correction term developed by Brandani (2004).

Figure 1 shows the experimental results and the fit of the adsorption data using a simple Langmuir isotherm. The isotherm parameters are listed in Table 1. Up to

25% CO_2 the flowrate correction procedure yields the same equilibrium properties for both adsorption and desorption experiments, confirming that N_2 is not adsorbed strongly. For the highest concentration the difference between adsorption and desorption results is due to the amount of carrier gas adsorbed in the column, and further experiments either with helium as a carrier or at higher concentrations would allow to determine the binary isotherm parameters, but this would be beyond the scope of the present contribution.

3. Breakthrough Simulation

3.1. Individual Channel Model

Ahn and Brandani (2004a) have developed a full 3-D mathematical model for a square channel and showed that, by a simple redistribution of the solid from the four corners to the four sides, it is possible to define an equivalent one dimensional diffusional resistance in the solid. To obtain the numerical solution to the full 3-D model on a high end PC several hours are required. Ahn and Brandani (2004b) have shown that it is possible to match exactly the 3-D simulation results using a 1-D model of adsorption between two parallel plates, by appropriately defining the equivalent dimension of the system. This reduces the computational time for a single channel breakthrough to one second or less (Ahn and Brandani, 2004b), thus allowing to model more rigorously a real monolith.

To develop the 1-D mathematical model the following assumptions were made: (i) isothermal condition,

Table 1. Monolith parameters.

Length of the total monolith column, L (m)	0.5
Length of each section of the column (m)	0.1
Cross-sectional Area (mm^2)	660
Average void fraction, ε (—)	0.6827
Diffusivity in gas phase, D_g (m^2/s)	$1.7 \cdot 10^{-5}$
Diffusivity in solid phase, D_s (m^2/s)	$3.3 \cdot 10^{-9}$
Height of the central channels, h_{avel} , and standard deviation, σ_l (mm)	1.38 ± 0.007
Height of the lateral channels, h_{aves} , and standard deviation, σ_s (mm)	1.0 ± 0.008
Wall half-thickness, w_{ave} , and standard deviation, σ_w (mm)	0.14 ± 0.0015
Viscosity of nitrogen at 298 K and 1 atm, η (μP)	177
N_2 volumetric flowrate (mm^3/s)	8333
Langmuir isotherm parameter, q_s (mmol/cm^3)	1.1532
Langmuir isotherm parameter, b (cm^3/mmol)	38.503

(ii) dispersed plug flow, (iii) the effect of nitrogen adsorption is negligible.

The component mass balance and the overall mass balance in the gas phase for an individual channel are

$$\frac{\partial c}{\partial t} - D_g \frac{\partial^2 c}{\partial z^2} + \frac{\partial (v_{ave} c)}{\partial z} + \frac{1 - \varepsilon}{\varepsilon} \frac{\partial \bar{q}}{\partial t} = 0 \quad (1)$$

$$\varepsilon c_{tot} \frac{\partial v_{ave}}{\partial z} + (1 - \varepsilon) \frac{\partial \bar{q}}{\partial t} = 0 \quad (2)$$

where c is the concentration in the gas phase, v_{ave} is the average velocity, \bar{q} is the average concentration in the solid phase.

The Langmuir isotherm and an LDF approximation are used for the estimation of equilibrium isotherm and adsorption kinetics, respectively.

$$q^* = \frac{q_s bc}{1 + bc} \quad (3)$$

$$\frac{\partial \bar{q}}{\partial t} = \frac{3D_s}{w_c^2} (q^* - \bar{q}) \quad (4)$$

where the corrected wall thickness for a square channel, which takes into account the contributions from the four corners, is given by Ahn and Brandani (2004a)

$$w_c = w(1 + w/h) \quad (5)$$

where h is the channel dimension and w is the wall half-thickness.

3.2. Modelling the Monolith Structure

The carbon monolith column is composed of a bundle of square channels as shown in Fig. 2. From the image it

is possible to determine that there are two characteristic channel sizes corresponding to the central region and the outer section of the monolith. Figure 2 was used to determine the relative occurrence, 1:9, of these channels as well as estimates of the variance of the channels sizes and wall thicknesses.

The structure of the monolith is described using Gaussian distributions for channel size and the wall thickness, characterised by an average value and a standard deviation.

$$D_{ch} = 0.9 \left(\frac{1}{\sqrt{2\pi}\sigma_l} \exp \left(-\frac{1}{2\sigma_l^2} (h - h_{ave})^2 \right) \right) + 0.1 \left(\frac{1}{\sqrt{2\pi}\sigma_s} \exp \left(-\frac{1}{2\sigma_s^2} (h - h_{aves})^2 \right) \right) \quad (6)$$

$$D_w = \frac{1}{\sqrt{2\pi}\sigma_w} \exp \left(-\frac{1}{2\sigma_w^2} (w - w_{ave})^2 \right) \quad (7)$$

The parameters used in Eqs. (6) and (7) are listed in Table 1. To limit the range of the size distributions, an upper and lower bound was chosen for w and h and the distribution functions were normalized into the probability functions, P_{ch} and P_w .

From the combined probability function, the void fraction of each channel and the cross-sectional area of the column, it is possible to derive the theoretical number of channels for the monolith

$$N_C = \frac{A}{\int_{w_{min}}^{w_{max}} \int_{h_{min}}^{h_{max}} P_{ch} P_w \frac{h^2}{\varepsilon} dh dw} \quad (8)$$

With the parameter values in Table 1, the estimated number of channels is 249, which is in close agreement with number of channels of the monolith, 247.

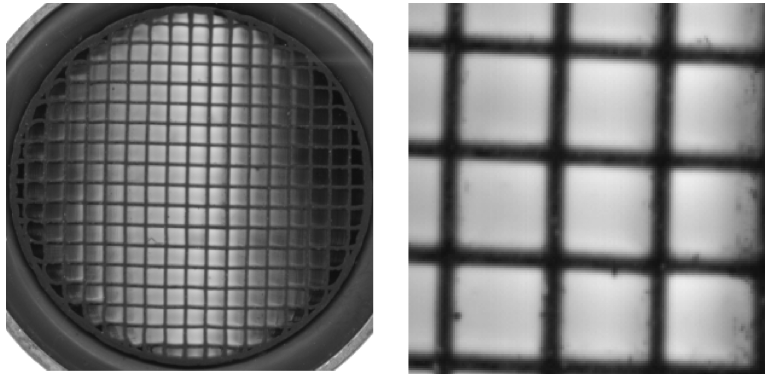


Figure 2. Cross section of the carbon monolith and detail of the central region.

While the variance of the wall thicknesses introduces range of diffusional time constants, which yield a broader breakthrough curve, the effect of the channel size becomes apparent when considering the gas velocity in the individual channels. The pressure drop across the monolith is very low, approximately 230 Pa in the range of flowrates of this study, but to model the system it is necessary to determine the velocity in the individual channels, using the relationship between pressure drop and average velocity for a square channel (Cornish, 1928).

$$v_{ave} = -\left(\frac{0.562 h^2}{16}\right) \frac{\Delta P}{\eta} \quad (9)$$

Equation (9) is used to determine iteratively ΔP from the known total gas flowrate and fluid viscosity η

$$Q = N_C \cdot \int_{h_{min}}^{h_{max}} P_{ch} \cdot v_{ave} \cdot h^2 dh \quad (10)$$

Having determined the average pressure drop, the inlet gas velocity can be calculated from Eq. (9).

The system of partial differential and algebraic equations coupled with the probability functions were coded in gPROMS (PSE, 1999) to obtain a numerical model for the individual monolith section. The column, consisting of 5 individual sections, was described using four connecting perfectly mixed sections representative of the spacers used in the column. Typical simulation times are approximately 1–2 hours.

The average concentration and adsorbed amount over all the channels were obtained from

$$c_{ave} = \frac{\int_{h_{min}}^{h_{max}} \int_{w_{min}}^{w_{max}} c v_{ave} h^2 P_{ch} P_w dw dh}{\int_{h_{min}}^{h_{max}} \int_{w_{min}}^{w_{max}} v_{ave} h^2 P_{ch} P_w dw dh} \quad (11)$$

$$\bar{q}_{ave} = \frac{\int_{h_{min}}^{h_{max}} \int_{w_{min}}^{w_{max}} \bar{q} P_{ch} P_w dw dh}{\int_{h_{min}}^{h_{max}} \int_{w_{min}}^{w_{max}} P_{ch} P_w dw dh} \quad (12)$$

4. Result and Discussion

Figure 3 shows representative comparisons of experimental breakthrough curves and predictions based on the detailed structure model and the equivalent single channel approach. The model that includes the detailed structure of the monolith provides an excellent match to both adsorption and desorption experimental results at different concentrations. The model based on the equivalent single channel approach incorrectly

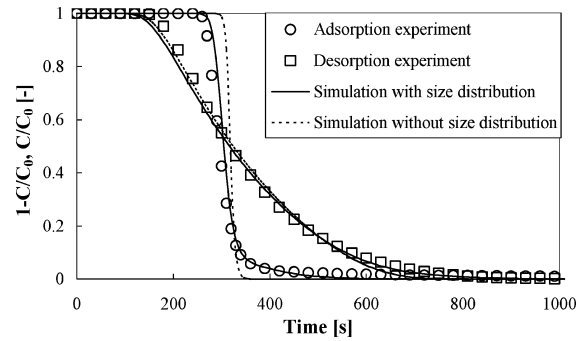


Figure 3. Results of adsorption and desorption breakthrough simulations at 25% CO₂, 298 K and ambient pressure.

predicts higher separation efficiencies for both concentrations. This is clearly evident from the predictions of the breakthrough times for the very sharp adsorption runs, where the single channel model is not able to reproduce the distinct broadening of the concentration front. This is true even for a monolith that appears to be nearly homogeneous, as can be seen in Fig. 2, and the performance of this monolith is reduced by combined effect of the smaller channels near the edge and the effect of small variations in the wall thicknesses coupled to the high solid phase mass transfer resistance.

The proposed model allows the prediction of process performance from kinetic and structural parameters that can be determined independently. Therefore, the model can provide an insight into ways to improve the design of monoliths and their packing into columns in order to optimise process performance.

5. Conclusions

The prediction of the dynamics of carbon dioxide breakthrough in a carbon monolith has been shown to require a detailed mathematical model that takes into account the real structure of the packing material. The model has been extended to include non-linear adsorption, which has been characterised experimentally using a procedure to determine the adsorption isotherm over a wide range of CO₂ concentrations, which does not require breaking the monolith. Future work will be aimed at extending the equilibrium results to binary systems and to investigate the dispersion in a monolith under flow reversal conditions.

Acknowledgments

Financial support from the Leverhulme Trust, Philip Leverhulme Prize, and Post-doctoral Fellowship Program of Korea Science & Engineering Foundation (KOSEF), is gratefully acknowledged. We are grateful to Dr. John Glomb, formerly of Mead-Westvaco Corporation for provision of the carbon monoliths.

References

- Ahn, H. and S. Brandani, "Analysis of Breakthrough Dynamics in Rectangular Channels of Arbitrary Aspect Ratio," *AIChE J.*, accepted for publication (2004a).
- Ahn, H. and S. Brandani, "A Detailed Model for the Prediction of Breakthrough Dynamics in Monoliths," in preparation (2004b).
- Brandani, S., "On the Chromatographic Measurement of Equilibrium Isotherms Using Large Concentration Steps," *Adsorption*, **11**, 231–235 (2005).
- Brandani, F., A. Rouse, S. Brandani, and D. M. Ruthven, "Adsorption Kinetics and Dynamic Behaviour of a Carbon Monolith," *Adsorption*, **10**, 99–109 (2004).
- Cornish, R.J., "Flow in a Pipe of Rectangular Cross-Section," *Proc. R. Soc.*, **120**, 691–700 (1928).
- Golay, M.J.E., *Theory of Chromatography in Open and Coated Tubular Columns with Round and Rectangular Cross-Sections*, in *Gas Chromatography*, D.H. Desty, (Ed.), Academic Press, New York, 1958, pp. 36–55.
- Process Systems Enterprise Ltd., *gPROMS Introductory User Guide* (1999).
- Ruthven, D.M. and C. Thaeron, "Performance of a Parallel Passage Adsorbent Contactor," *Gas Separation and Purification*, **10**, 63–73 (1996).
- Ruthven, D.M., "Past Progress and Future Challenges in Adsorption Research," *Ind. Eng. Chem. Res.*, **39**, 2127–2131 (2000).